Out-of-Surveillance Target State Estimation: A Combined Hospitability and Synthetic Inclination Approach

Zaher M. Kassas, Ümit Özgüner, and Jeff Layne

***Abstract*— This paper presents a novel approach for estimating out-of-surveillance mobile ground target states. The proposed algorithm introduces the concepts of hospitability and synthetic inclination maps and embeds them into a nonlinear Bayesian estimation filter, which in turn produces optimal target state estimates for a given out-of-surveillance mobile ground target of interest. The optimality criterion here is defined in the minimum mean square error sense. Loosely speaking, the hospitability map can be viewed as a terrain-based map defining a likelihood or a "weight" for each point on the earth's surface proportional to the ability of the target to move and maneuver at that location. On the other hand, the synthetic inclination map describes how the target favors certain regions within the search area, hence being "synthetically" inclined to move towards them.**

I. INTRODUCTION

In this work, the following problem is studied: in a given search area, an aerial uninhibited autonomous vehicle (UAV) detects a mobile target using its own sensor(s). While the target is being detected, the UAV makes several observations on the target. The proposed estimation algorithm employs the knowledge gained from the first set of observations taken by the UAV and the concepts of hospitability maps (HMaps) and synthetic inclination maps (SIMaps) embedded into an nonlinear Bayesian estimation filter to estimate target states when it goes out-of-surveillance. Loosely speaking, the HMap can be viewed as a terrain-based map defining a likelihood or a "weight" for each point on the earth's surface proportional to the ability of the target to move and maneuver at that location. In contrast, the SIMap describes how the target favors certain regions within the search area, hence being "synthetically" inclined to move towards them [1].

The rest of this paper is organized as follows. Section II presents an optimal nonlinear Bayesian estimation filter design. Section III introduces the concepts of HMaps and SIMaps. Section IV defines a combined HMap and SIMap cost function and couples it with the optimal nonlinear Bayesian filter derived in Section II. Section V presents some simulations and results. Concluding remarks and future work are discussed in Section VI.

This work was supported by the AFRL/VA and AFOSR Collaborative Center of Control Science F33615-01-2-3154.

Z. M. Kassas is with the Department of Electrical and Computer Engineering, The Ohio State University, 2015 Neil Ave., Columbus, OH 43210, USA zkassas@ieee.org

Ü. Özgüner is with the Faculty of the Department of Electrical and Computer Engineering, The Ohio State University, 2015 Neil Ave., Columbus, OH 43210, USA ozguner.1@osu.edu

J. Layne is with The Air Force Research Laboratory, 2241 Avionics Circle WPAFB, Ohio 45433-7318 Jeffery.Layne@wpafb.af.mil

II. OPTIMAL NONLINEAR BAYESIAN ESTIMATION FILTER DESIGN

The target dynamics will be modeled by the Itô stochastic differential equation, given by

$$d\mathbf{x}(t) = \mathbf{F}[\mathbf{x}(t), t]dt + G[\mathbf{x}(t), t]d\beta(t),\ t \in [t_0, T], \quad (1)$$

where $\mathbf{x}(t)^1 \in \mathbb{R}^n$ is the target state vector, $\mathbf{F}[\mathbf{x}(t), t]^2 \in \mathbb{R}^n$, $G[\mathbf{x}(t), t] \in \mathbb{R}^{n\times r}$, and $\{\beta(t), t \geq t_0\} \in \mathbb{R}^r$ is a vector of independent Brownian motion processes with $E\{d\beta(t)d\beta^{\mathrm{T}}(t)\} = Q(t)dt$. It is worth noting that (1) is *formally* equivalent to the Langevin equation

$$\dot{\mathbf{x}}(t) = \mathbf{F}[\mathbf{x}(t), t] + G[\mathbf{x}(t), t]\eta(t), \quad (2)$$

where $\mathbf{x}(t)$, $\mathbf{F}[\mathbf{x}(t), t]$, and $G[\mathbf{x}(t), t]$ are defined as before, and $\eta(t) \in \mathbb{R}^r$ is a zero-mean white Gaussian noise process with an autocorrelation function $Q(t)\delta(t-\tau)$, where $Q(t) \in \mathbb{R}^{r\times r}$ is the covariance matrix of the noise process, and $\delta(t)$ is the Dirac delta function.

The UAV makes observations on this target that are taken at discrete-time instants t_k according to

$$\mathbf{z}_{t_k} = \mathbf{H}[\mathbf{x}_{t_k}, t_k] + \mathbf{v}_{t_k}, \qquad k = 0, 1, 2, \ldots, \quad (3)$$

where $\mathbf{z}_{t_k} \in \mathbb{R}^m$ is the observation vector, $\mathbf{H}[\mathbf{x}_{t_k}, t_k] \in \mathbb{R}^m$, and $\mathbf{v}_{t_k}$ is a zero-mean white Gaussian noise process with covariance matrix $R_{t_k} \in \mathbb{R}^{m\times m} > 0$.

It will be assumed that the initial probability density function (pdf) of the SDS defined in (1) is known and that it is once continuously differentiable with respect to time, t, and twice continuously differentiable with respect to the state variable, $\mathbf{x}(t)$. In addition, it will be assumed that the linear/nonliear function $\mathbf{H}[\mathbf{x}_{t_k}, t_k]$ in (3) is continuous in both arguments and bounded for each t_k with probability 1. Moreover, the initial state $\mathbf{x}(t_0)$, the system noise $\eta(t)$, and the measurement noise $\mathbf{v}_{t_k}$ are assumed to be all independent. Finally, it will be assumed that (1) has a solution on $[t_0, T]$ in the mean square sense [2].

Given this SDS definition with the stated assumptions, it can be shown that between observations, the conditional pdf $p\left[\mathbf{x}(t), t|\mathbf{Z}_{t_k}\right]$ [3] satisfies the Fokker-Planck-Kolmogorov Equation (FPKE) [2], that is described by the *diffusion* process given by the partial differential equation

[1] $\mathbf{x}(t) = [x_1(t), x_2(t), \ldots, x_n(t)]^{\mathrm{T}}$
[2] $\mathbf{F}[\mathbf{x}(t), t] = [f_1[\mathbf{x}(t), t], f_2[\mathbf{x}(t), t], \ldots, f_n[\mathbf{x}(t), t]]^{\mathrm{T}}$
[3] $\mathbf{Z}_{t_k} \triangleq \{\mathbf{z}_{t_k}, \mathbf{Z}_{t_{k-1}}\}$

$$\frac{\partial}{\partial t}p = -\sum_{i=1}^{n}\frac{\partial}{\partial x_i}\{pf_i\} + \frac{1}{2}\sum_{i=1}^{n}\sum_{j=1}^{n}\frac{\partial}{\partial x_i \partial x_j}\{p(GQG^{\mathrm{T}})_{ij}\}, \quad (4)$$

where the following short-hand notation has been used in (4): $p = p\left[\mathbf{x}(t), t|\mathbf{Z}_{t_{k-1}}\right]$, $f_i = f_i[\mathbf{x}(t), t]$, $G = G[\mathbf{x}(t), t]$, and $Q = Q(t)$.

Whenever a new observation, $\mathbf{z}_{t_k}$, at time t_k becomes available, the conditional pdf $p\left[\mathbf{x}(t), t|\mathbf{Z}_{t_{k-1}}\right]$ needs to be updated to the new pdf $p\left[\mathbf{x}(t), t|\mathbf{Z}_{t_k}\right]$. This can be accomplished by applying Bayes' rule, given as

$$p\left[\mathbf{x}(t), t|\mathbf{Z}_{t_k}\right] = \frac{p\left[\mathbf{x}(t), t|\mathbf{Z}_{t_{k-1}}\right] p\left[\mathbf{z}_{t_k}|\mathbf{x}(t)\right]}{\int p\left[\mathbf{x}(t), t|\mathbf{Z}_{t_{k-1}}\right] p\left[\mathbf{z}_{t_k}|\mathbf{x}(t)\right] d\mathbf{x}(t)} \quad (5)$$

where the term $p\left[\mathbf{z}_{t_k}|\mathbf{x}(t)\right]$ in (5) can be evaluated from

$$p\left[\mathbf{z}_{t_k}|\mathbf{x}(t)\right] = \frac{1}{(2\pi)^{\frac{m}{2}}\left|R_{t_k}\right|^{\frac{1}{2}}} \mathrm{e}^{-\frac{1}{2}\left[\mathbf{z}_{t_k}-\mathbf{H}\right]^{\mathrm{T}} R_{t_k}^{-1}\left[\mathbf{z}_{t_k}-\mathbf{H}\right]}, \quad (6)$$

where $\mathbf{H} = \mathbf{H}[\mathbf{x}_{t_k}, t_k]$. Essentially, (4) and (5) constitute the predictor and corrector equations, respectively, of the nonlinear Bayesian estimation filter. The mean of the conditional pdf in (5) with respect to the state variable yields the optimal minimum mean square error (MMSE) estimates, i.e.

$$\hat{\mathbf{x}}(t) = \int_{-\infty}^{\infty} \mathbf{x}(t) p\left[\mathbf{x}(t), t|\mathbf{Z}_{t_k}\right] d\mathbf{x}(t). \quad (7)$$

The nonlinear Bayesian estimation filter just defined generally possesses two undesirable characteristics: infinite-dimensionality and difficulty to achieve a closed-form analytical solution for higher-dimensional complicated FPKE's. These two issues are dealt with separately next.

A. Adaptive state variable domain truncation

Optimal nonlinear filters are generally said to be infinite-dimensional filters. This implies that some form of state variable domain truncation would be necessary, when numerical techniques are employed. The most common approach for domain truncation adopted in literature is to set the domain limits very wide in order to ensure that the significant mass of the pdf would lie within these preset limits at all time [3]. However, in most practical applications this would burden the filter with exhaustive computations that would contribute too little to the overall mass of the pdf. To overcome the computational burden without sacrificing the estimation accuracy, adaptive state variable domain truncation algorithm has been proposed [1], [4], [5].

The algorithm of adaptive state variable domain truncation basically incorporates the Chebyshev Inequality Theorem along with the moment evolution theorem to "optimally adjust and truncate" the state variable domain limits, and hence the pdf size. This adjustment and truncation ensures that the significant mass of the pdf would lie within these limits at every time step, while not degrading the accuracy of the estimates.

The Chebyshev Inequality Theorem [6], also known as the Chebyshev Bound (C.B.), states that given an arbitrary random variable x, with mean $E\{x\}$, and finite variance σ_x^2; then, for any $\lambda > 0$

$$\begin{aligned} P\{|x - E\{x\}| \geq \lambda\sigma_x\} &\leq \frac{1}{\lambda^2} \\ \Rightarrow P\{|x - E\{x\}| < \lambda\sigma_x\} &\geq 1 - \frac{1}{\lambda^2}. \end{aligned} \quad (8)$$

Equation (8) may be viewed as the probability of a realization of the random variable x to lie within the interval $(E\{x\} - \lambda\sigma_x, E\{x\} + \lambda\sigma_x)$ to be bounded by $1 - \frac{1}{\lambda^2}$.

The Union Bound states that given *n*-events $\{E_1, E_2, \ldots, E_n\}$ (not necessarily disjoint), the probability of the union of these events is less than or equal to the summation of the events' individual probabilities [6], i.e.

$$P\left\{\bigcup_{i=1}^{n} E_i\right\} \leq \sum_{i=1}^{n} P\{E_i\}. \quad (9)$$

Using the Union Bound, the C.B. can be generalized to the case of *n*-random variables $[x_1, x_2, \ldots, x_n]$, with respective means $[E\{x_1\}, E\{x_2\}, \ldots, E\{x_n\}]$ and respective variances $\left[\sigma_{x_1}^2, \sigma_{x_2}^2, \ldots, \sigma_{x_n}^2\right]$ as

$$P\left\{\bigcup_{i=1}^{n}\left[|x_i - E\{x_i\}| < \lambda_i\sigma_{x_i}\right]\right\} \geq 1 - \varepsilon, \quad (10)$$

where ε is the design parameter to be selected, given by

$$\varepsilon = \sum_{i=1}^{n}\frac{1}{\lambda_i^2}. \quad (11)$$

There are two approaches for solving for ε, one is based on other Chebyshev-type inequalities, and the other is based on use of weighted values of λ's [7]. The approach employed in the simulations presented in this paper is to select $\lambda_1 = \lambda_2 = \ldots \equiv \lambda$, which is rationalized by the fact that the σ-limits of all the state variables are of equal importance, and thus no preferred weighting is given to one state variable on the expense of the other.

In order to adaptively find the optimal state variable domain limits, the present and future domain limits need to be calculated. The union of these limits yields the optimal state variable domain for the complete time pdf evolution. Since at a given time step the current pdf is available, finding the first and second moments is straightforward. However, at a given time step, the future evolving pdf is unknown; hence, the future first and second moments cannot be computed as directly. Nevertheless, future first and second moments may still be optimally predicted through the moment evolution theorem.

The moment evolution theorem states that given a SDS characterized by (1) and observations made on this system according to (3), and under some boundedness, Lipschitzanity, and independence hypotheses and assumptions [2], then between observations, the conditional mean vector and covariance matrix of the pdf $p\left[\mathbf{x}(t), t|\mathbf{Z}_{t_k}\right]$ satisfy

1) Mean evolution:

$$\frac{d}{dt}E\left\{\mathbf{x}(t)\right\} = E\left\{\mathbf{F}[\mathbf{x}(t), t]\right\}. \qquad (12)$$

2) Covariance evolution:

$$\begin{aligned} \frac{d}{dt}P(t) &= \left[E\left\{\mathbf{x}\mathbf{F}^{\mathrm{T}}\right\} - E\left\{\mathbf{x}\right\}E^{\mathrm{T}}\left\{\mathbf{F}\right\}\right] \\ &\quad + \left[E\left\{\mathbf{F}\mathbf{x}^{\mathrm{T}}\right\} - E\left\{\mathbf{F}\right\}E^{\mathrm{T}}\left\{\mathbf{x}\right\}\right] \\ &\quad + \left[E\left\{GQG^{\mathrm{T}}\right\}\right], \qquad (13) \end{aligned}$$

where the following short-hand notation has been used in (13): $\mathbf{x} = \mathbf{x}(t)$, $\mathbf{F} = \mathbf{F}[\mathbf{x}(t), t]$, $G = G[\mathbf{x}(t), t]$, and $Q = Q(t)$. Actually, it was shown in [1] that in certain cases we need not evolve the entire covariance matrix, since computing only the diagonal terms of the matrix would suffice. This reduces the number of computations from $n + n^2$ to $2n$.

B. Numerical solutions to the FPKE

Generally, it is extremely difficult to obtain a closed-form analytical solution to the FPKE [8]. Two of the commonly used methods to solve the FPKE numerically are finite element methods and finite difference methods. In this paper, finite difference method will be presented.

In the finite difference method, the time and state variable domains are discretized and defined over a finite number of equally-spaced grid points. Consequently, the partial derivatives are evaluated at each of the grid points/cells, which are represented as $(x_j, t_i) = (j\Delta x, i\Delta t)$, $1 \leq j \leq k+1$, and $i \geq 0$; where $k \in \mathbb{N}$, Δx is the discretization step in the state variable domain, and Δt is the discretization step in time. The following finite difference approximations can be used to approximate the solution of the FPKE in (4)

$$\begin{aligned} \frac{\partial f\left(x,t\right)}{\partial t}\Big|_{t=t_i} &= \frac{A}{\Delta t} \qquad (14) \\ \frac{\partial f\left(x,t\right)}{\partial x}\Big|_{t=t_{i-1}} &= \frac{B}{2\Delta x} \qquad (15) \\ \frac{\partial^2 f\left(x,t\right)}{\partial x^2}\Big|_{t=t_{i-1}} &= \frac{C}{(2\Delta x)^2}, \qquad (16) \end{aligned}$$

where

$$\begin{aligned} A &= f\left(x, t_i\right) - f\left(x, t_{i-1}\right) \\ B &= f\left(x_{j+1}, t_{i-1}\right) - f\left(x_{j-1}, t_{i-1}\right) \\ C &= f\left(x_{j+1}, t_{i-1}\right) - 2f\left(x_j, t_{i-1}\right) + f\left(x_{j-1}, t_{i-1}\right). \end{aligned}$$

The stability condition for the explicit finite difference method states that the grid spacings in the time domain and the state variable domain must satisfy the inequality

$$0 < \Delta t \sum_{i=1}^{n} \frac{1}{\left(\Delta x_i\right)^2} \leq \frac{1}{2}, \qquad (17)$$

where Δx_i is the grid spacing of the $i^{th}-$state variable.

III. THE HOSPITABILITY MAP (HMAP) AND THE SYNTHETIC INCLINATION MAP (SIMAP)

The earth's surface is rarely *flat* and *unvarying* in a given search area of large enough dimensions. Hence, it is quite logical to assume that the different terrain a search area may exhibit should influence where and how the target moves at a specific locale. This motivates introducing the concept of the HMap to constrain the search area into regions of higher/lower hospitability for a given class of targets. In [9], Layne et. al. defined the HMap as a map providing a likelihood or a "weight" for each point on the earth's surface proportional to the ability of a target to move and maneuver at that location. The following factors are considered while deriving the hospitability value: slope, surface roughness, transportation, geology, landform, soil, vegetation, hydrology, urban areas, and climate. Additionally, the HMap is a function of the nature of the target itself, i.e. there exists different models for deriving the HMap for different classes of targets (eg. cars, tanks, amphibious vehicles, etc.) [10]. A generic HMap is illustrated in Fig. 1, where the HMap values has been normalized to lie in the interval $[0, 1]$, with 1 being the highest hospitability index.

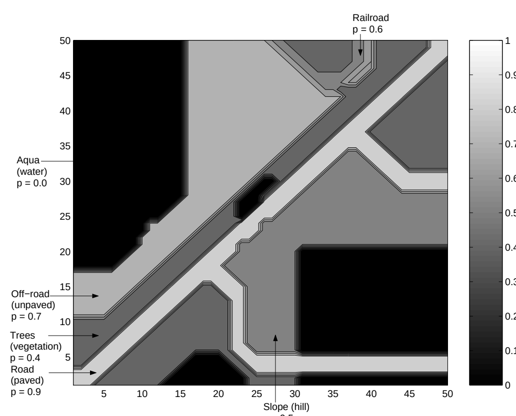

Fig. 1. A Generic HMap

We now introduce the concept of the SIMap, which is a function of the velocity components, and hence the heading of the target. Specifically, the SIMap is a two-dimensional (2-D) velocity map in $(\dot{x}, \dot{y})$ defined for each 2-D point (x, y) describing that given the target is located at a particular point (x_0, y_0) how would the target be *synthetically inclined* to move in different directions with certain velocity components. Therefore, whence the HMap is a function of the nature of the target and the topography of the search area, the SIMap is a function of the nature of the target as well as how the target "favors" different zones within the search area.

Fig. 2 shows a simple way of looking at SIMaps. In a given search area $\mathcal{S}$, we assume that we are given a priori estimates about the target initial position, denoted by (x_0, y_0). Additionally, we will assume that within $\mathcal{S}$, there is a zone Ω where the target is interested to head towards *as fast as possible*. Hence, we say that the target is *synthetically inclined* to move towards Ω. Consequently, we may define a weighting function that assigns a "weight" for each of the velocity component combinations the target may have.

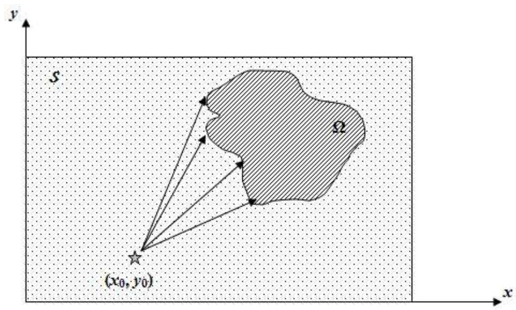

Fig. 2. SIMap Illustration

The construction of SIMaps depends on several factors. The nature of the target itself is one important factor in determining the velocity components domain the target may have. For instance, if the target under consideration is a tank with a maximum speed s_{max}, then we can safely assign the SIMap domain to take positive and negative values of $(\dot{x}, \dot{y})$ satisfying the inequality $\sqrt{(\dot{x})^2 + (\dot{y})^2} \leq s_{max}$. Another consideration affecting the construction of SIMaps is to subdivide the search area into different zones, such as zones where the target would like to reach as fast as possible, zones where the target would like to escape from as fast as possible, zones where the target would like to stay stationary at (eg. hiding regions), and zones where the target would have different $\dot{x}$ and $\dot{y}$ velocity components (eg. roads and railroads) [1].

IV. Coupling the Nonlinear Estimation Filter with the HMap and SIMap

This section will integrate the concepts that have been developed in Sections II and III. First, we will combine the HMap and the SIMap into one 4-D map in $(x, y, \dot{x}, \dot{y})$. The combined HMap-SIMap may be understood by fixing the 2-D (x, y) coordinates at a particular point (x_0, y_0) and varying the velocity components $(\dot{x}, \dot{y})$ over the domain they may take. To illustrate this concept, let's assume that the velocity components are restricted to the discrete values $[-3, -2, -1, 0, +1, +2, +3]$. Consequently, each fixed point in the 2-D HMap layer will be associated with a 2-D SIMap layer as demonstrated in Fig. 3. Note that the origin of the SIMap in Figure 3 is the fixed point (x_0, y_0). Note also that there are 7^2 different velocity components combinations the target may have, each represented by a vector with corresponding magnitude and direction.

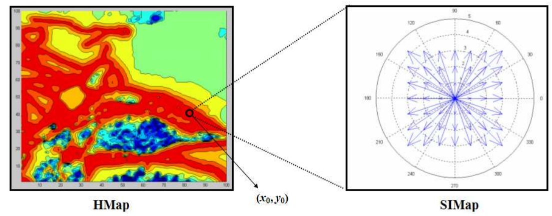

Fig. 3. Relationship between the HMap and SIMap Layers

Next, we will couple the combined 4-D HMap-SIMap with the nonlinear Bayesian estimation filter that was derived in Section II. The problem statement can be reiterated as follows. We want to estimate the target state vector, defined as the target Cartesian $x-$ and $y-$position and velocity $\mathbf{x}(t) = [x(t), y(t), \dot{x}(t), \dot{y}(t)]^{\mathrm{T}}$, for mobile out-of-surveillance ground targets. Now, whenever a UAV detects a mobile target via its onboard sensors, the nonlinear Bayesian estimation filter should take over and produce optimal target state estimates. However, once the target goes out-of-surveillance, the filter cannot update the pdf anymore, and we will define the following update equation

$$p^+(t = i, \mathbf{x}) = \frac{1}{a} p^-(t = i, \mathbf{x}).c^{-1}(\mathbf{x}), \qquad (18)$$

where $p^+(t = i, \mathbf{x})$ is the updated pdf at time $t = i$, $p^-(t = i, \mathbf{x})$ is the un-updated pdf at time $t = i$, a is a normalizing constant, and $c(\mathbf{x})$ is the combined HMap-SIMap cost function. The cost function $c(\mathbf{x})$ is essentially a 4-D array, defined for all 4-D points $\mathbf{x}_0$, where $\mathbf{x}_0$ is the state vector $\mathbf{x}$ evaluated at a particular 4-D point $\mathbf{x}_0$. In particular, $\mathbf{x}_0 = [x_0, y_0, \dot{x}_0, \dot{y}_0]^{\mathrm{T}}, \forall (x_0, y_0) \in \mathcal{S}$ and $\forall (\dot{x}_0, \dot{y}_0) \in [-v_{max}, +v_{max}]$, with $\mathcal{S}$ being the search area under consideration and v_{max} being the maximum $x-$ or $y-$velocity component the target may have.

The inverse of the cost function $c(\mathbf{x})$ will be defined as a linear combination of the hospitability weight and the negative exponential of the Euclidean norm between a given point $\mathbf{x}'_0 = (x_0 + \dot{x}_0, y_0 + \dot{y}_0)$ and a boundary condition (final point) $\mathbf{x}_f = (x_f, y_f)$. In particular, $c(\mathbf{x})$ will be defined as

$$c^{-1}(\mathbf{x}_0) = \alpha H(x_0, y_0) + \beta \, \mathrm{e}^{-\delta} \qquad (19)$$

$$\delta = ||\mathbf{x}_f - \mathbf{x}'_0|| \qquad (20)$$

$$= \sqrt{[x_f - (x_0 + \dot{x}_0)]^2 + [y_f - (y_0 + \dot{y}_0)]^2},$$

where α and β are weighting scalars, $\mathbf{x}_0$ is the 4-D point defined previously, $H(x_0, y_0)$ is the hospitability weight at $\mathbf{x}_0$, and $\delta = ||\mathbf{x}_f - \mathbf{x}'_0||$ is the Euclidean norm between the final point $\mathbf{x}_f$ and the point the target would reach if it moves from (x_0, y_0) with velocity components $(\dot{x}_0, \dot{y}_0)$.

Note that the weighting scalars α and β can be selected according to the respective weighting we want to associate the hospitability term with versus the inclination term.

Fig. 4 summarizes the algorithm for estimating the states of an out-of-surveillance mobile target. Note the optimization block, which essentially implements the adaptive state variable domain truncation to reduce the computational burden to the "minimum". Note also that the filter switches between two modes. If the target is being detected by the UAV, then the filter would update the pdf through the new observations made on the target, whereas if the target is out-of-surveillance then the filter would update the pdf through the HMap-SIMap updating algorithm presented in this section.

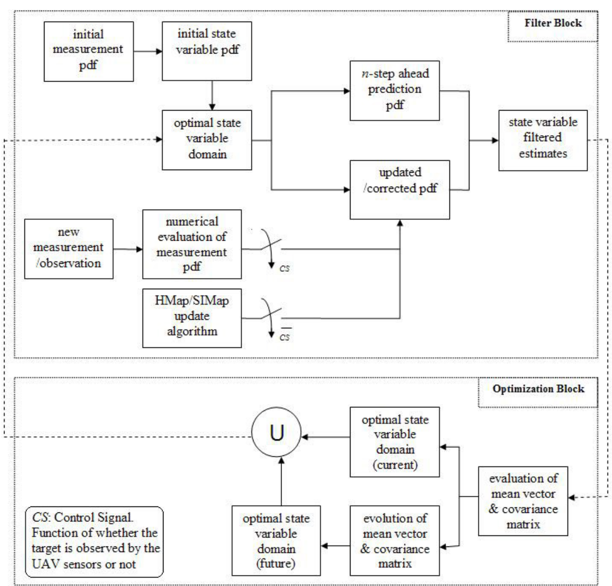

Fig. 4. Filter Block Diagram

V. Simulations and Results

This section summarizes some of the results achieved upon running simulations to demonstrate the ideas presented in this work. The target was considered to be moving in a linear trajectory on the 2-D xy-plane according to the linear motion model with nearly constant velocity, where the acceleration is modeled as a stationary white Gaussian noise. The target states were defined to be the Cartesian $x-$ and $y-$position and velocity. Therefore, the corresponding vectors and matrices defined in (1) simplify to

$$\mathbf{x}(t) = \begin{bmatrix} x(t) \\ y(t) \\ \dot{x}(t) \\ \dot{y}(t) \end{bmatrix}, \qquad \mathbf{F}[\mathbf{x}(t), t] = \begin{bmatrix} \dot{x}(t) \\ \dot{y}(t) \\ 0 \\ 0 \end{bmatrix}$$

$$G[\mathbf{x}(t), t] = \begin{bmatrix} 0 & 0 \\ 0 & 0 \\ 1 & 0 \\ 0 & 1 \end{bmatrix}, \qquad Q(t) = \begin{bmatrix} q^2 & 0 \\ 0 & q^2 \end{bmatrix}.$$

The UAV may detect the target if the target falls within a predefined rectangular footprint of the UAV sensors and provide measurements of the range r and the bearing angle ϕ, both corrupted by additive white Gaussian noise. Hence, given that the UAV is located at (x_u, y_u, z_u) and the target is located at $(x_t, y_t, 0)$, the corresponding vectors and matrices defined in (3) simplify to

$$\mathbf{z}_{t_k} = \begin{bmatrix} r_{t_k} \\ \phi_{t_k} \end{bmatrix}, \qquad R_{t_k} = \begin{bmatrix} \sigma_r^2 & 0 \\ 0 & \sigma_\phi^2 \end{bmatrix},$$

$$\mathbf{H}[\mathbf{x}(t), t] = \begin{bmatrix} \sqrt{(x_u - x_t)^2 + (y_u - y_t)^2 + z_u^2} \\ \tan^{-1}\left[\frac{y_u - y_t}{x_u - x_t}\right] \end{bmatrix}.$$

Two scenarios have been simulated on the filter derived in this paper. The first scenario assumed that the mobile target is falling within the footprint of the UAV sensors. Hence, the UAV was capable of producing observations on the target (switch CS in Fig. 4 being closed). These noisy observations were filtered through the estimation filter and the mean square estimation error (MSEE) for both the $x-$ and $y-$ position of the target are plotted in Fig. 5 and Fig. 6, respectively. In order to demonstrate the accuracy of the state estimates of the optimal nonlinear stochastic Bayesian filter derived, an Extended Kalman Filter (EKF) for the same particular problem was derived and simulated with the same set of noisy measurements. The $x-$ and $y-$position MSEE of the EKF estimates are superimposed on the plots of Figures 5 and 6, respectively. The superiority of the nonlinear Bayesian filter estimates versus their EKF counterparts can be easily noted.

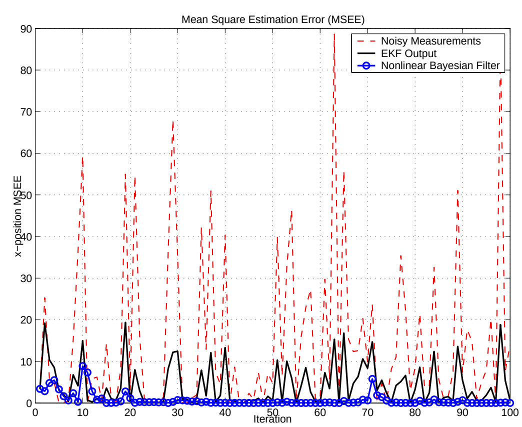

Fig. 5. MSEE in the x-position

The second scenario assumed that the target would go out-of-surveillance after it has been initially detected by the UAV sensors. Hence, the switch CS in Fig. 4 opens and the pdf is now being updated through the HMap-SIMap updating algorithm. The HMap employed for these set of simulations was the one shown in Fig. 1. The location at which the target was last detected by the UAV sensors was at $(15, 15)$ and we assumed that the target was interested to head towards the boundary point $(40, 40)$. Two cases

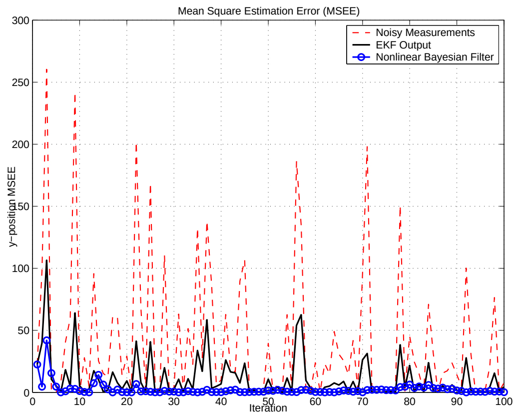

Fig. 6. MSEE in the y-position

have been studied. The first case propagated the pdf in the proposed filter for 40 iterations, but the cost function consisted of the HMap term alone. The second case propagated the same pdf in the proposed filter for 40 iterations, but the cost function consisted of both the HMap and SIMap terms. Fig. 7 and Fig. 8 illustrate the resulting pdf's. It can be seen clearly that the the pdf resulting from the incorporation of the HMap term alone yielded a pdf that is splitting at the junction of the two roads, since they are both less costly (as hospitable) for the pdf to propagate through. However, when incorporating the HMap term along with the SIMap term, the pdf did not split into the two junctions, since the SIMap term was *redirecting* the pdf to move towards the boundary point rather than merely following the hospitable cells in the search area. Hence, we conclude that the incorporation of the SIMap term along with the HMap term in the cost function would yield more robust estimates whenever a junction of road segments and/or a junction of relatively equally hospitable regions are present in the search area.

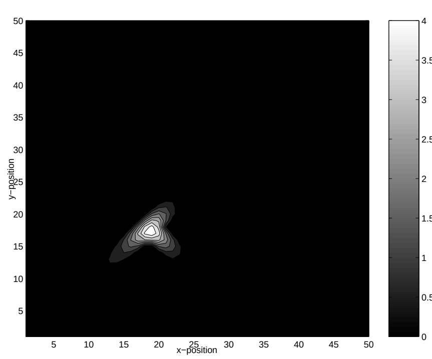

Fig. 7. Pdf Propagation of Target Position with HMap Term Alone

VI. CONCLUSIONS AND FUTURE WORKS

This paper has presented a novel approach for estimating the states of an out-of-surveillance mobile target. Essentially, this work has extended the filter proposed by Layne et. al. in [9] into a more robust filter by introducing the

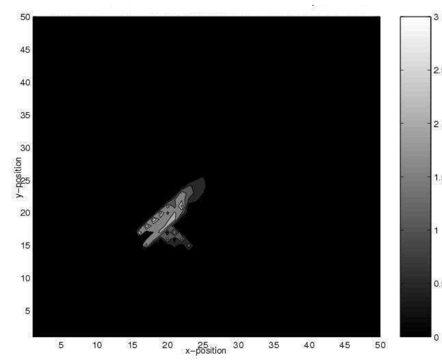

Fig. 8. Pdf Propagation of Target Position with HMap & SIMap Terms

concept of SIMaps. In addition, an optimization algorithm has been derived in order to reduce the computational load burden of the nonlinear Bayesian filter to the "minimum", while not degrading the estimation accuracy. Further research is suggested in the area of constructing SIMaps. In particular, further research would be necessary to construct SIMaps such that the boundary point is extended to a boundary surface. In addition, further research is necessary to construct and simulate SIMaps for the case where several regions are present within the search area. Finally, the authors believe that the concept of limited-memory filters, which are usually adopted whenever the SDS dynamics are not precisely known would be useful to implement within the nonlinear Bayesian estimation filter derived in this work, if the target dynamics are not precisely defined.

REFERENCES

[1] Z. M. Kassas, "An optimal nonlinear bayesian filter design and combined hospitability and synthetic inclination approach for tracking and estimation," Master of Science Thesis, The Ohio State University, Columbus, OH, 2003.

[2] A. H. Jazwinski, *Stochastic Processes and Filtering Theory*. New York, NY: Academic Press, 1970.

[3] B. T. Park, "Stochastic acceleration in electron-dominated solar flares," Ph.D. dissertation, Dept. of Physics, Stanford University, Stanford, CA, Jul. 1996.

[4] A. Challa and Y. Bar-Shalom, "Nonlinear filter design using fokker-planck-kolmogorov probability density equations," *IEEE Transactions on Aerospace and Electronic Systems*, vol. 36, no. 1, pp. 309–315, Jan. 2000.

[5] S. Challa and F. A. Faruqi, "Application of chebechev's inequality theorem in the design of optimal non-linear filters," in *ICASSP, Proceedings of the 1998 IEEE International Conference on Acoustics, Speech, and Signal Processing'98*, May 1998, pp. 1277–1280.

[6] H. Stark and J. W. Woods, *Probability and Random Processes with Applications to Signal Processing*, 3rd ed. Upper Saddle River, NJ: Prentice Hall, 2002.

[7] S. Challa, "Nonlinear state estimation and filtering with applications to target tracking," Ph.D. dissertation, Signal Processing Research Center, Queensland University of Technology, Australia, Oct. 1998.

[8] H. Risken, *The Fokker-Planck Equation*. Berlin: Springer-Verlag, 1989.

[9] J. Layne, M. Eilders, Z. M. Kassas, and U. Ozguner, in *Recent Developments in Cooperative Control and Optimization*, S. Butenko, R. Murphey, and P. M. Pardalos, Eds. Boston: Kluwer Academic Publishers, 2003, pp. 117–124.

[10] J. D. Priddy, "Stochastic vehicle mobility forecasts using the nato reference mobility model," US Army Corps of Engineers, Tech. Rep. 3, 1995.